Articles

Structure, Single Crystal EPR Spectra, and Exchange Interactions in $[Cu(L\text{-proline})_2]_2\cdot 5H_2O$ and $Cu(D,L\text{-proline})_2\cdot 2H_2O$

R. P. Sartoris, L. Ortigoza, N. M. C. Casado, and R. Calvo*

Departamento de Física, Facultad de Bioquímica y Ciencias Biológicas, Universidad Nacional del Litoral, and INTEC (CONICET-UNL), Güemes 3450, 3000 Santa Fe, Argentina

E. E. Castellano

Instituto de Física de São Carlos, Universidade de São Paulo, C. P. 369, 13560 São Carlos SP, Brazil

O. E. Piro

Departamento de Física, Facultad de Ciencias Exactas, Universidad Nacional de La Plata and Programa PROFIMO (CONICET), C.C. 67, 1900 La Plata, Argentina

Received January 20, 1999

A new copper(II) compound, $[Cu(L\text{-proline})_2]_2\cdot 5H_2O$ ($C_{20}Cu_2H_{42}N_4O_{13}$) (called compound **I**) was synthesized and crystallized, and its structure was solved using X-ray methods. It is monoclinic, space group $P2_1$, with $a = 11.187(1)$ Å, $b = 12.172(3)$ Å, $c = 11.661(1)$ Å, $\beta = 114.96(1)°$, and $Z = 2$. There are two chemically different copper molecules (labeled A and B), both with the copper atom in a N_2O_2 square planar coordination. Molecule type A has one water molecule in an apical position. Molecule B has water molecules in each of the two apical positions. Single-crystal EPR measurements have been performed in **I** and also in $Cu(D,L\text{-proline})_2\cdot 2H_2O$ (compound **II**). From the similar angular variations of the position of the single resonance observed in both compounds, we evaluated the molecular **g** tensors. Interpretation of the molecular **g** tensors resulted in $d_{x^2-y^2}$ orbital ground states. From the angular variations of the line width we calculated the magnitude of the exchange interactions coupling neighbor copper ions in each compound. In **I** copper ions type A at 7.25 Å are arranged in chains coupled through axial−equatorial bonds. The exchange coupling within these chains is $|J/k| = 118$ mK. The coupling between copper ions type B is weaker. However, the interactions between copper ions type A and B generate a three-dimensional magnetic network. Our data in compound **II** indicate that a superexchange pathway containing a weak hydrogen bond C−H- - -O is the path for an exchange interaction with $|J'/k| = 48$ mK between coppers in neighbor layers at 9.75 Å.

Introduction

The metal coordination in metal-amino acid compounds has received much attention because they are simple systems to study the coordination of these ions in metaloproteins. Their crystal structures,[1] optical properties,[2] electronic structure, and magnetic properties[3−10] have been studied. They are relatively easy to synthesize and crystallize, and several different techniques have been applied to these compounds in order to elucidate various aspects of metal coordination in biomolecules. The magnetic properties of metal amino acid compounds are also interesting from their own. Due to their structures and to the properties of the bonds, they show low-dimensional magnetism at low temperatures[3−6] with phase transitions to magnetically ordered phases below 1 K.[3,6]

We are interested in the magnetic interactions between metal ions or metal ions and radicals produced in metaloproteins during the biological cycle. The magnitudes of the exchange interactions are related to properties of the bonds connecting the unpaired spins and may provide structural information not readily available from X-ray crystallographic data. Dipolar interactions are directly related to the structure. Within this perspective, metal amino acid complexes are also attractive as model systems for the magnetic interactions. To elucidate the role of biologically relevant molecular fragments as paths for the transmission of exchange interactions we have studied several metal-amino acid compounds. A careful analysis of single-crystal EPR data and the crystal structure allow us to

---

* Corresponding author. Fax: +54 (342) 455 0944. E-mail: rcalvo@dfbioq.unl.edu.ar.

(1) Freeman, H. C. in *Inorganic Biochemistry*; Eichhorn, G. L., Ed.; Elsevier: Amsterdam, 1973; Chapter 3 and references therein.

(2) Graddon, D. P.; Munday, L. *J. Inorg. Nucl. Chem.* **1960**, *23*, 231.

(3) Newman, P. R.; Imes, J. L.; Cowan, J. A. *Phys. Rev. B* **1976**, *13*, 4093.

(4) Calvo, R; Passeggi, M. C. G.; Novak, M. A.; Symko, O. G.; Oseroff, S. B.; Nascimento, O. R.; Terrile, M. C. *Phys. Rev. B* **1991**, *43*, 1074.

(5) Siqueira, M. L.; Rapp, R. E.; Calvo, R. *Phys. Rev. B* **1993**, *48*, 3257.

(6) Rapp, R. E.; Souza, E. P.; Godfrin, H.; Calvo, R. *J. Phys.: Condens. Matter* **1995**, *7*, 9595.

10.1021/ic9900758 CCC: $18.00

determine the relative efficiencies of intermolecular exchange through different pathways in the crystal. Our studies provided estimations of the (small) magnitudes of superexchange transmitted along carboxylate bridges,[7] hydrogen bonds,[5] and long σ bonds.[8,9] These values were analyzed in terms of the structural information.

In this work we investigate two copper complexes of the amino acid proline. The structure of $Cu(D,L\text{-proline})_2 \cdot 2H_2O$ (compound **II**) was reported by Mc L. Mathieson and Welsh,[11] and by Shamala et al.[12] Recently it was redetermined with higher precision by Hitchman et al.,[10] who also reported the molecular **g** tensor from a single-crystal EPR experiment. To compare magnetic properties of pairs of copper(II) complexes with L-amino acids and with their racemic mixtures[5,13,14] we also synthesized and grew single crystals of $[Cu(L\text{-proline})_2]_2 \cdot 5H_2O$ (compound **I**). The crystal structure of this new compound was determined and a detailed electron paramagnetic resonance (EPR) study of oriented single-crystal samples of compounds **I** and **II** was performed. Our data are used to describe the electronic state of the Cu(II) ions and to evaluate exchange interactions between pairs of copper ions in each compound. In compound **I** we estimate the magnitude of the exchange interaction transmitted by a path containing five diamagnetic atoms. In $Cu(D,L\text{-proline})_2 \cdot 2H_2O$ (**II**) it allows us to determine the role of a superexchange path containing a weak hydrogen bond in the transmission of the exchange interaction.

Experimental Section

Materials. The compound $[Cu(L\text{-proline})_2]_2 \cdot 5H_2O$ (**I**) was obtained from the reaction of L-proline with basic copper carbonate in water. The solubility of this compound is high in water but low in organic solvents. Single crystals grow in a 9:1 acetone/water solution, in acetone atmosphere. Blue rectangular prisms of about 0.5×3×0.5 mm, elongated along the *b* axis and showing *ab* and *bc* lateral faces were obtained in few days.

The solubility in water of $Cu(D,L\text{-proline})_2 \cdot 2H_2O$ (**II**) is smaller than that for compound **I**. So, single crystals were obtained by slow evaporation of a water solution at room temperature. Blue rectangular prismatic crystals elongated along the *a* axis, showing lateral *ab* and *ac* faces, of about 2×1×0.1 mm, grew in few days.

Single crystals of each compound were glued to cubic sample holders made of cleaved KCl crystals, which define a set *x*, *y*, *z* of orthogonal axes. The *a* and *b* axes of each sample were accurately aligned along the *x* and *y* axes of the holders, respectively. Therefore, $c' = a \times b$ is along the ***z*** axis of each sample holder. This procedure reduces the difficulties of handling the samples during the EPR measurements and allows the orientation uncertainties to be reduced to about 1°.

Crystallographic Measurements. A prismatic crystal of 0.1×0.1×0.4 mm of compound **I** was mounted in an Enraf-Nonius CAD-4 diffractometer. The unit cell dimensions and the orientation matrix for the collections of the diffraction data were obtained by least-squares refinement of $(\sin \theta/\lambda)^2$ for 25 centered reflections in the $14.0 < \theta < 15.2$ range. The diffraction intensities were measured with the $\omega - 2\theta$ scan technique with speeds between 2.85 and 20.0°/min, determined from a previous scan at 20°/min. Reflections in the interval $0 < \theta < 25°$ were collected using graphite-monochromated Mo Kα radiation. From 2446 independent reflections measured, 1833 have $I > 3\sigma(I)$, with $\sigma(I)$ calculated from the counting statistics. Table 1 gives the crystallographic data. Table S1 in the Supporting Information includes more experimental details. Diffraction data were corrected by Lorentz, polarization, and absorption effects.[15] In our calculation we used the atomic dispersion coefficients of Cromer and Waber[16] and the anomalous dispersion coefficients of Cromer and Ibers.[17] These calculations were performed with the SHELX[18] and SDP[19] systems of programs.

Table 1. Crystallographic Data for Compounds $[Cu(L\text{-proline})_2]_2 \cdot 5H_2O$ (**I**) and $Cu(D,L\text{-proline})_2 \cdot 2H_2O$ (**II**)

	I	**II**[a]
molecular formula	$C_{20}H_{42}Cu_2N_4O_{13}$	$C_{10}H_{20}CuN_2O_6$
M	673.66	327.8
crystal class	monoclinic	monoclinic
space group	$P2_1$	$P2_1/n$
a/Å	11.187(1)	5.579(1)
b/Å	12.172(3)	17.903(5)
c/Å	11.661(1)	7.003(2)
β/deg	114.96(1)	104.53(3)
V/Å^3	1496	677.2
D_x/g cm^{-3}	1.554	1.61
Z	2	2
F(000)	694	342
μ(Mo Kα)/cm^{-1}	23.47	17.0
specimen/mm	0.1 × 0.1 × 0.4	0.30 × 0.05 × 0.25
$2\theta_{\max}$/deg	25	60
N	1950	1992
N_0 $[I > 3\sigma(I)]$	1509	1334
R	0.038	0.036
R'	0.040	0.048

[a] From ref 10.

EPR Measurements. EPR data in single crystals were obtained at 9.7 GHz and room temperature with a Bruker ER-200 EPR spectrometer, using a 12″ rotating magnet, and a Bruker cylindrical cavity with 100 kHz field modulation. The sample holders for each sample were positioned in a horizontal plane at the top of a pedestal, in the center of the microwave cavity. The magnetic field **B** was rotated in the *xy*, *zx*, and *zy* planes of the samples, and the spectra were recorded at intervals of 10°. The EPR signal was collected digitally as a function of **B**. Positions and line widths of these signals were obtained by fitting the spectra with field derivatives of Lorentzian line shapes.

Crystallographic Results

$[Cu(L\text{-proline})_2]_2 \cdot 5H_2O$. The structure of $[Cu(L\text{-proline})_2]_2 \cdot 5H_2O$ was solved using direct and Fourier methods and refined by least squares, blocking adequately molecular fragments with anisotropic thermal parameters for all non-hydrogen atoms. A Fourier difference map calculated at this stage showed a substantial part of the H atoms of the proline ligands, and eight hydrogens from the five hydration water molecules. These last ones were incorporated stereochemically in the final molecular model together with the hydrogens of the prolines with a common thermal parameter which was adjusted to the value $U = 0.13$ Å[16] during the final refinement process.

Table 2 gives the fractional atomic coordinates of the non-hydrogen atoms of $[Cu(L\text{-proline})_2]_2 \cdot 5H_2O$ (**I**). As shown in Figure 1, there are two copper molecules in different crystallographic sites (labeled A and B). Both have the copper atom

---

(7) Levstein, P. R.; Calvo, R. *Inorg. Chem.* **1990**, *29*, 1581.
(8) Brondino, C. D.; Casado, N. M. C.; Passeggi, M. C. G.; Calvo, R. *Inorg. Chem.* **1993**, *32*, 2078.
(9) Calvo, R.; Steren, C. A.; Piro, O. E.; Rojo, T.; Zuniga, F. J.; Castellano, E. E. *Inorg. Chem.* **1993**, *32*, 6016.
(10) Hitchman, M. A.; Kwan, L.; Engelhardt L. M.; White, A. H. *J. Chem. Soc., Dalton Trans,* **1987**, 457.
(11) McL Mathieson, A.; Welsh, H. K. *Acta Crystallogr*. **1952**, 5, 599.
(12) Shamala, N.; Venkatesan, K. *Cryst. Struct. Commun*. **1973**, *2*, 5.
(13) Levstein, P. R.; Calvo, R.; Castellano, E. E.; Piro, O. E.; Rivero, B. E. *Inorg. Chem.* **1990**, *29*, 3918.
(14) Levstein, P. R.; Pastawski, H. M.; Calvo, R. *J. Phys.: Condens. Matter* **1991**, *3*, 1877.
(15) Busing, W. R.; Levy, H. A. *Acta Crystallogr.* **1957**, *10*, 180.
(16) Cromer, D. T.; Waber, J. T. in *International Tables for X-ray Crystallography*; Kynoch Press: Birmingham, 1974; Vol. IV, p 71.
(17) Cromer, D. T.; Ibers, J. A. In *International Tables for X-ray Crystallography*; Kynoch Press: Birmingham, 1974; Vol. IV, p 149.
(18) Sheldrick, G. M. *SHELX: A Program for Crystal Structure Determination*; University of Cambridge: Cambridge, UK, 1976.
(19) Frenz, B. A. *Enraf-Nonius Structure Determination Package*; Enraf-Nonius: Delft, The Netherlands, 1983.

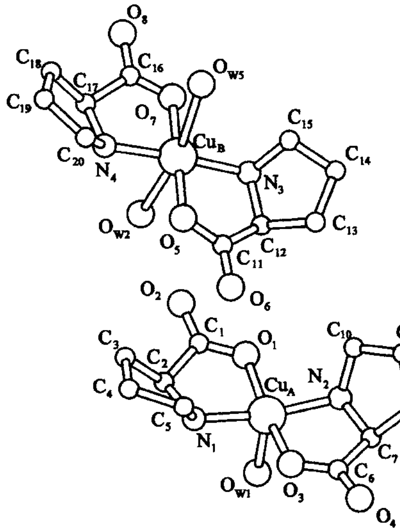

Figure 1. Molecular structure of [Cu(L-proline)$_2$]$_2$·5H$_2$O (**I**). Pairs of L-proline molecules are bonded to the two chemically different copper ions in the unit cell.

Table 2. Positional Parameters for [Cu(L-proline)$_2$]$_2$·5H$_2$O

atom	*x*	*y*	*z*
CuA	0.4353(1)	0.5000(0)	0.3149(1)
N1	0.5998(5)	0.5021(6)	0.2897(5)
O1	0.5173(5)	0.6201(5)	0.4333(5)
O2	0.6879(6)	0.7318(5)	0.5034(6)
C1	0.6308(8)	0.6491(6)	0.4446(7)
C2	0.6976(7)	0.5747(8)	0.3849(7)
C3	0.765(1)	0.640(1)	0.312(1)
C4	0.720(1)	0.5842(9)	0.1883(9)
C5	0.5841(9)	0.5424(8)	0.1625(7)
N2	0.2605(6)	0.5295(5)	0.3146(5)
O3	0.3370(5)	0.4063(5)	0.1695(5)
O4	0.1420(7)	0.3363(7)	0.0565(6)
C6	0.2177(9)	0.3919(8)	0.1426(7)
C7	0.1626(8)	0.4499(8)	0.2251(8)
C8	0.043(1)	0.518(1)	0.150(1)
C9	0.074(1)	0.632(1)	0.202(2)
C10	0.2111(9)	0.6426(8)	0.2719(9)
CuB	0.6121(1)	1.0761(1)	0.2665(1)
N3	0.4527(6)	1.0312(6)	0.2910(5)
O5	0.5675(6)	0.9547(5)	0.1487(5)
O6	0.4401(7)	0.8066(6)	0.0852(7)
C11	0.4762(8)	0.8920(7)	0.1490(7)
C12	0.4097(7)	0.9224(7)	0.2324(7)
C13	0.2582(9)	0.9318(8)	0.159(1)
C14	0.222(1)	1.036(1)	0.208(1)
C15	0.337(1)	1.1044(8)	0.234(1)
N4	0.7835(6)	1.1081(5)	0.2620(6)
O7	0.6597(5)	1.1927(6)	0.3923(5)
O8	0.7975(7)	1.3276(5)	0.4736(7)
C16	0.7638(7)	1.2417(6)	0.4123(7)
C17	0.8547(8)	1.1910(8)	0.3589(8)
C18	0.916(2)	1.270(1)	0.300(2)
C19	0.897(1)	1.224(1)	0.180(1)
C20	0.790(1)	1.1411(9)	0.1406(9)
Ow1	0.5078(5)	0.3593(5)	0.4628(5)
Ow2	0.7644(6)	0.9346(5)	0.4615(5)
Ow3	0.0339(6)	0.4180(5)	0.6144(6)
Ow4	0.1959(6)	0.3535(6)	0.8482(6)
Ow5	0.5053(8)	1.2474(7)	0.1184(7)

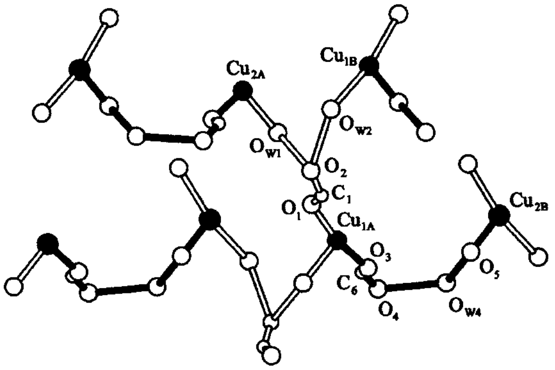

Figure 2. Main interaction paths between copper ions in [Cu(L-proline)$_2$]$_2$·5H$_2$O (**I**).

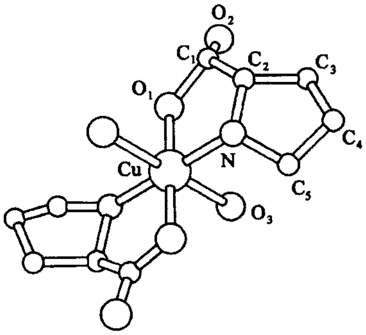

Figure 3. Coordination around copper ions in Cu(D,L-proline)$_2$·2H$_2$O (**II**) showing L-proline and D-proline molecules and the square planar arrangement of N$_2$ O$_2$ ligands (from ref 10).

trans-coordinated to two proline molecules in a N$_2$O$_2$ square planar arrangement (average distances Cu−O = 1.947 Å, Cu−N = 1.987 Å). Type A molecule is monohydrated [Cu(L-proline)$_2$·H$_2$O], with the water molecule in one apical position (distance Cu−Ow$_1$ = 2.321 Å). Type B molecule is dihydrated [Cu(L-proline)$_2$·2H$_2$O] with the two water molecules in opposite apical positions (distances Cu−Ow$_2$ = 2.788 Å and Cu−Ow$_5$ = 2.649 Å). The angle between the normals to the equatorial planes of Cu(A) and Cu(B) sites is 14.5°. There are two symmetry-related sites (1 and 2) for each chemically different copper ion (A and B) in the unit cell. The angle between the normals to the symmetry-related sites is $2\alpha = 86.3°$ for the pair $1_A{-}2_A$ and $2\alpha = 100.2°$ for the pair $1_B{-}2_B$, with an average value $2\alpha = 93.25°$.

In compound **I** Cu(1_A) and Cu(2_A) at 7.25 Å, are connected through [Cu(1_A)−O−C=O(2)- - -H−Ow$_1$−Cu(2_A)] axial−equatorial pathways giving rise to Cu(1_A)−Cu(2_A)−Cu(1_A) chains (Figure 2). The coupling between copper type B molecules is weaker. However, the chemical bridges [Cu(1_A)−O−C=O(4)- - -H−Ow$_4$−H−O(5)−Cu(2_B)] and [Cu(1_B)−Ow$_2$−H- - -O(2)=C−O−Cu(1_A)] between Cu(A) and Cu(B), provide the coupling between Cu(A) chains, and give rise to a three-dimensional exchange network, respectively.

Cu(D,L-proline)$_2$·2H$_2$O. The structure of Cu(D,L-proline)$_2$·2H$_2$O (compound **II**) is known.[10−12] Each Cu(II) ion is located in a center of symmetry, trans-coordinated to one L-proline and one D-proline molecules with a N$_2$O$_2$ square planar arrangement of ligands and two water molecules occupying axial positions (Figure 3). There are two symmetry-related molecules (1 and 2) in the unit cell of this compound and the angle between their apical directions is $2\alpha = 99.28°$. The coordination of the copper sites and the orientation of the apical ligands relative to the *abc′* crystal axis system is similar in compounds **I** and **II** (see Figure 4). As shown later, this is reflected by the EPR data.

The copper atoms in Cu(D,L-proline)$_2$·2H$_2$O (**II**) are arranged in layers parallel to the *ac′* plane. Each layer contains one type of copper ions (1 or 2) at an average distance of 6.25 Å. These layers are distributed in an alternating sequence at 9.75 Å. The chemical bridges [Cu(1)−O(3)- - -H−C(4)−C−N−Cu(2)] connecting rotated copper ions in neighbor layers are shown in Figure 5. This path involves five diamagnetic atoms including a weak hydrogen bond between O(3) and C(4) at a distance of 3.68 Å. There are not other paths which may transmit the

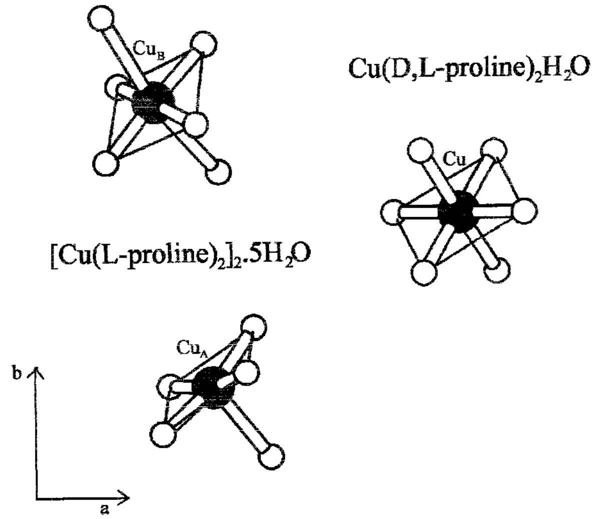

Figure 4. Orientation to the apical ligands relative to the *abc′* crystal axis system in [Cu(L-proline)$_2$]$_2$•5H$_2$O (**I**) and Cu(D,L-proline)$_2$•2H$_2$O (**II**), respectively.

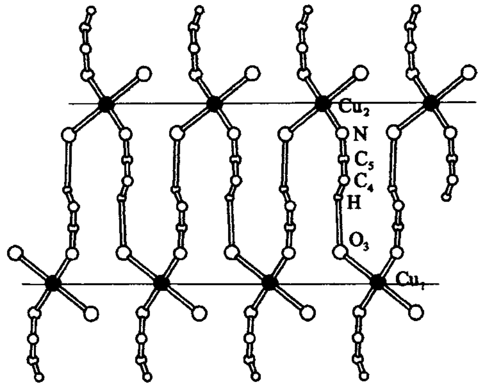

Figure 5. Projection along the ***c*** axis of the Cu(D,L-proline)$_2$•2H$_2$O (**II**) crystal lattice showing the exchange paths connecting coppers in different layers, which contain C−H- - -O bonds.

exchange interaction $J' = J_{1-2}$ between rotated copper ions in neighboring layers.

EPR Results and Analysis

Crystal g^2 Tensors. A single exchange-collapsed EPR line was observed for any orientation of the applied field **B** in both compounds. These are "crystal resonances" attributed to the coupled spin systems. They arise from the collapse of the resonances corresponding to the magnetically nonequivalent sites in the unit cells of [Cu(L-proline)$_2$]$_2$•5H$_2$O (**I**) (4 sites) and Cu(D,L-proline)$_2$•2H$_2$O (**II**) (2 sites) produced by the exchange interactions. To analyze the data we introduce the spin-Hamiltonian:

$$H = \mu_B\, \mathbf{S}\cdot\mathbf{g}\cdot\mathbf{B} \tag{1}$$

where **S** is the effective spin ($S = {}^1/_2$), $\mathbf{B} = B\mathbf{h}$, is the external magnetic field applied along $\mathbf{h} = \mathbf{B}/|\mathbf{B}|$, **g** is the tensor describing the angular variation of the **g** factor, and μ_B is the Bohr magneton. For an arbitrary direction of **h**, the squared **g** factor calculated from eq 1 is

$$g^2(\theta,\phi) = \mathbf{h}\cdot\mathbf{g}\cdot\mathbf{g}\cdot\mathbf{h} = (g^2)_{xx}\sin^2\theta\cos^2\phi + (g^2)_{yy}\sin^2\theta\sin^2\phi + (g^2)_{zz}\cos^2\theta + 2(g^2)_{xy}\sin^2\theta\sin\phi\cos\phi + 2(g^2)_{xz}\sin\theta\cos\theta\cos\phi + 2(g^2)_{zy}\sin\theta\cos\theta\sin\phi \tag{2}$$

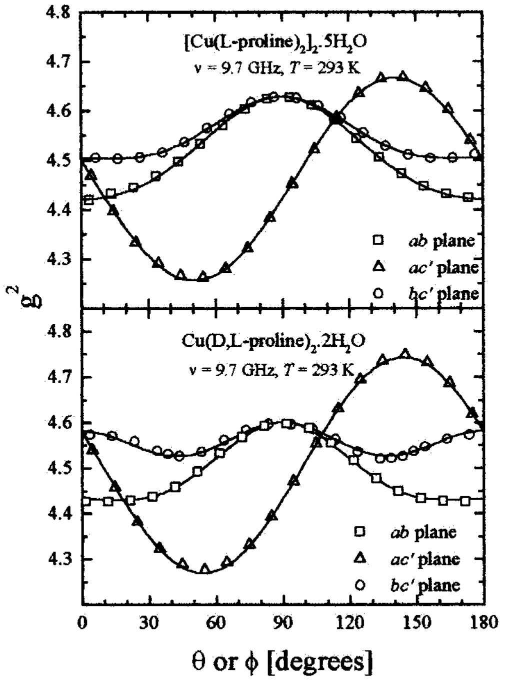

Figure 6. Angular variation of g^2 (θ,ϕ) at 9.7 GHz and 293 K for the magnetic field applied in the *ab*, *ac′*, and *bc′* crystalline planes of the single crystal of [Cu(L-proline)$_2$]$_2$•5H$_2$O (**I**) and Cu(D,L-proline)$_2$•2H$_2$O (**II**). The solid lines are obtained using eq 2 and the parameters given in Table 3.

Figure 6 displays the observed angular variation of the squared **g** factor in three orthogonal planes of [Cu(L-proline)$_2$]$_2$•5H$_2$O (**I**) and Cu(D,L-proline)$_2$•2H$_2$O (**II**). These results, eq 2, and a least-squares procedure were used to calculate the components of the **g**^{2} tensor for each compound in the $xyz \equiv abc'$ system of axes. These values are given in Table 3, and the solid lines in Figure 6 are calculated with these components.

In [Cu(L-proline)$_2$]$_2$•5H$_2$O (**I**) the orientation of the symmetry axis of the 1A site is close to that of the 1B site. This orientation also resembles that of the A site in compound **II**. This explains the similarity of the **g**^{2} tensors of compounds **I** and **II** shown in Figure 6 and Table 3.

Molecular g^2 Tensors. In a system where the resonances due to nonequivalent spins in the lattice are fully collapsed by the exchange, the crystal **g**^{2} tensor defined in eq 1 is the average of the molecular **g**^{2} tensors of the individual sites.[20] For [Cu(L-proline)$_2$]$_2$•5H$_2$O (compound **I**) we have

$$\mathbf{g}^2 = [\mathbf{g}_{1,A}{}^2 + \mathbf{g}_{1,B}{}^2 + \mathbf{g}_{2,A}{}^2 + \mathbf{g}_{2,B}{}^2]/4 \tag{3}$$

For Cu(D,L-proline)$_2$•2H$_2$O (compound **II**) it is

$$\mathbf{g}^2 = [\mathbf{g}_1{}^2 + \mathbf{g}_2{}^2]/2 \tag{4}$$

Information about the electronic structure of each copper site is contained in the molecular **g**^{2} tensors on the right side of eqs 3 and 4. They have six components for each chemically different copper in the lattice, a total of twelve values for compound **I** and six for compound **II**. The experimental results in Table 3 provide only four nonzero components of the average **g**^{2} tensor for each compound. Therefore, to calculate the components of the molecular tensors from the data we have to make assumptions. Several methods of calculation of the molecular **g** tensor from the experimental crystal **g** tensor have been proposed.[20−25]

---

(20) Abe, H.; Ono, K. *J. Phys. Soc. Jpn.* **1956**, *11*, 947.

Table 3. Values of the Components of the Crystal $\mathbf{g}^2$ Tensors Obtained by a Least-Squares Analysis of the Data[a]

	[Cu(L-proline)$_2$]$_2$·5H$_2$O	Cu(D,L-proline)$_2$·2H$_2$O
$(g^2)_{xx}$	4.421 (1)	4.431(1)
$(g^2)_{yy}$	4.628(1)	4.600(1)
$(g^2)_{zz}$	4.504(1)	4.581(1)
$(g^2)_{xz}$	−0.201(1)	−0.224(1)
$(g^2)_{xy} = (g^2)_{zy}$	0	0
$(g^2)_1$	4.257(1)	4.269(1)
$(g^2)_2$	4.667(1)	4.743(1)
$(g^2)_3$	4.628(1)	4.600(1)
$\mathbf{a}_1$	(0.77,0,0.63)	(0.812,0,0.584)
$\mathbf{a}_2$	(0.63,0,−0.77)	(0.584,0,−0.812)
$\mathbf{a}_3$	(0,1,0)	(0,1,0)
$\mathbf{g}_\perp$	2.063(1)	2.066(2)
$\mathbf{g}_\|$	2.245(1)	2.252(2)
2α, deg (from EPR)	92.89	100.2
2α, deg (from X-rays)	93.25	99.28
A_1	67(2) G	66(2) G
A_2	27(2) G	91(2) G
A_3	−37(4) G	−24(4) G
A_4	−240(10) G	−80(10) G
A_5	0.00080(7) G^{-1}	−
A_6	−	1300(100) G[b]

[a] g_1^2, g_2^2, and g_3^2 and $\mathbf{a}_1$, $\mathbf{a}_2$, and $\mathbf{a}_3$ are the eigenvalues and eigenvectors of the $\mathbf{g}^2$ tensors in the $xyz = abc'$. We include the values of $\mathbf{g}_\perp$, $\mathbf{g}_\|$ and the angle 2α between the normals to the square of ligands to copper ions calculated from the EPR data and the angle 2α obtained from the crystallographic data. The values of the coefficients A_i obtained by least-squares fits of eq 6 to the line width data for compounds **I** and **II** in Figure 7 are also included. [b] This coefficient, calculated from the approach used by Hitchman, is not substantially different.

The main difference is the proposed point symmetry of the metal site. The simplest approach is to assume axial symmetry around the ***z*** axis which under this approximation is coincident with the orientation of the apical ligands.[20−24] One may also assume that the direction connecting the metal ion with one of the equatorial ligands is a C_2 symmetry axis in a rhombic environment.[25] This approach was chosen by Hitchman et al. for Cu(D,L-proline)$_2$·2H$_2$O and other copper compounds.[10]

In the case of Cu(D,L-proline)$_2$·2H$_2$O (compound **II**) the copper ion site has only inversion symmetry. In [Cu(L-proline)$_2$]$_2$·5H$_2$O (compound **I**) the copper ion has not any point symmetry operation. Also, the angles L-Cu-L′ (where L and L′ are two consecutive equatorial ligands) are significantly different from 90° in both compounds. Thus, it is difficult to assume safely a given orientation for the eigenvectors of the **g** tensor. In this work we neglect these asymmetries assuming axial symmetry for the molecular **g** tensor $\mathbf{g}_{1,\mathrm{A}}$, $\mathbf{g}_{1,\mathrm{B}}$, $\mathbf{g}_{2,\mathrm{A}}$, $\mathbf{g}_{2,\mathrm{B}}$ (compound **I**) and $\mathbf{g}_1$ and $\mathbf{g}_2$ (compound **II**), with $\mathbf{g}_\perp$ in the plane of ligands and $\mathbf{g}_\|$ perpendicular to it. This approach is acceptable for the analysis of the line widths produced by the exchange interactions that is performed in the next section (see later). In addition, we assume that for [Cu(L-proline)$_2$]$_2$·5H$_2$O (compound **I**) the values of $\mathbf{g}_\perp$ and $\mathbf{g}_\|$ are equal for molecules A and B. Thus,

$$\mathbf{g}_{\perp\mathrm{A}} \cong \mathbf{g}_{\perp\mathrm{B}} \cong \mathbf{g} \text{ and } \mathbf{g}_{\|\mathrm{A}} \cong \mathbf{g}_{\|\mathrm{B}} \cong \mathbf{g}_\|$$

With these approximations, we calculated from our experimental data $\mathbf{g}_\perp$, $\mathbf{g}_\|$, and the average angle 2α between the apical directions of the rotated copper sites as in ref 23. These values are given in Table 3 which shows that the angle 2α calculated from the EPR data agrees well with that obtained from the structural data.

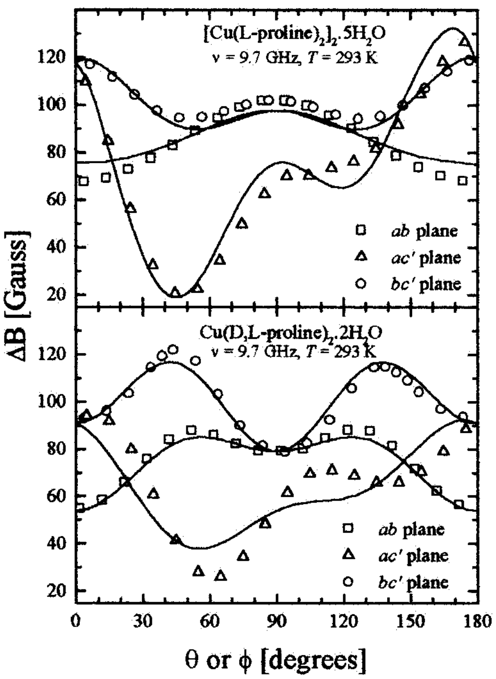

Figure 7. Angular variation of the peak-to-peak EPR line width observed at 9.7 GHz and 293 K, for the magnetic field applied in three crystalline planes of a single-crystal sample of [Cu(L-proline)$_2$]$_2$·5H$_2$O (**I**) and Cu(D,L-proline)$_2$·2H$_2$O (**II**). The solid lines are obtained using eq 6, and the parameters included in Table 3.

Line Width Data and Evaluation of the Exchange Interactions between Copper Ions. The angular variations of the resonance line width observed for compounds **I** and **II** are displayed in Figure 7. In all measurements the observed line shape was nearly Lorentzian, as expected for exchange-collapsed resonances.

To estimate the magnitudes of the exchange coupling between neighbor copper ions in compounds **I** and **II** from the line width data we write the exchange Hamiltonian as[26,27]

$$H_{\mathrm{ex}} = {}^1/_2\sum_{ij} J_{ij}^{11}\mathbf{S}_i^1\cdot\mathbf{S}_j^1 + {}^1/_2\sum_{ij} J_{ij}^{22}\mathbf{S}_i^2\cdot\mathbf{S}_j^2 + {}^1/_2\sum_{ij} J_{ij}^{12}\mathbf{S}_i^1\cdot\mathbf{S}_j^2 \quad (5)$$

where the superscripts 1 and 2 denote the two symmetry-related copper sites, which are magnetically nonequivalent for an arbitrary orientation of the applied field **B**, and i and j indicate different unit cells.

To perform a quantitative analysis, the peak-to-peak line width data for each compound displayed in Figure 7 were least-squares fitted with the angular function:[24]

$$\Delta B(\theta,\phi) = A_1 + A_2\cos^2\theta + A_3\sin\theta\cos\theta\cos\phi + A_4(\sin\theta\cos\theta\cos\phi)^2 + A_5M_2 + A_6[g_{\mathrm{A}}(\theta,\phi) - g_{\mathrm{B}}(\theta,\phi)]^2 \quad (6)$$

where θ and ϕ are referred to the crystal axes system abc' and M_2 is the second moment of the dipolar interaction which can be calculated from the crystal structure. In eq 6 A_1 is an isotropic

---

(21) Billing, D. E.; Hathaway, B. J. *J. Chem. Phys.* **1969**, *50*, 1476.

(22) Hathaway, B. J.; Billing, D. E. *Coord. Chem. Rev.* **1970**, *5*, 143 and references therein.

(23) Servant, I.; Bissey, J.S.; Maini, M. *Physica (Utrecht)* **1981**, *106B*, 343.

(24) Calvo, R.; Mesa, M. A. *Phys. Rev.* **1983**, *28*, 1244.

(25) Dawson, K.; Hitchman, M. A.; Prout, C. K.; Rossotti, F. J. C. *J. Chem. Soc., Dalton Trans.* **1972**, 1509.

(26) Calvo, R.; Isern, H.; Mesa, M. A. *Chem. Phys.* **1985**, *100*, 89.

(27) Gennaro, A. M.; Levstein, P. R.; Steren, C. A.; Calvo, R. *Chem. Phys.* **1987**, *111*, 431.

contribution to the line width, and A_2, A_3, and A_4 are small second-order contributions arising from interactions as hyperfine, antisymmetric and anisotropic exchange. The last two terms, A_5 and A_6 are due to dipolar and residual Zeeman interactions, respectively. They are the most important contributions to the angular variation of the line width, and reflect the differences between the exchange networks in compounds **I** and **II**. The values of the coefficients of eq 6 calculated from a fitting of the line width data in Figure 7 are given in Table 3. These values were obtained using the axial-symmetry approach previously discussed for the molecular g-tensors in the last term of eq 6. If the molecular **g** tensor of $Cu(\text{D,L-proline})_2 \cdot 2H_2O$ calculated by Hitchman et al.[10] assuming that the Cu−N direction is a C_2 axis is used in the last term in eq 6, the value of A_6 is very similar to our result in Table 3.

In $Cu(\text{D,L-proline})_2 \cdot 2H_2O$ (**II**) the principal contribution to the angular variation of the line width is given by the A_6 term and arise from the nonequivalence of the copper sites. This effect, called "residual Zeeman" contribution,[28] is clearly observed in the bc' plane (Figure 7), where the smallest line widths are for **B** along the crystal axes, where the resonances of the nonequivalent copper ions collapse by symmetry. The coefficient A_6 is related to the exchange frequency ω_{ex} by[28]

$$A_6 = \frac{\sqrt{(2\pi)^5/3}\ \nu^2\hbar}{4g^3\omega_{ex}^2\mu_B}$$

where ν is the microwave frequency. The exchange frequency ω_{ex} is related to the interlayer exchange-coupling parameter J' coupling nearest-neighbor nonequivalent copper ions, ($J' = J_{ij}$[12] in eq 5). It is $\omega_{ex}^2 = zJ'^2/\hbar^2$, where $z = 4$ is the number of nonequivalent neighbors (Figure 5).

In $[Cu(\text{L-proline})_2]_2 \cdot 5H_2O$ (**I**), the most important contribution to the angular variation of the line width is the A_5 term in eq 6 and is attributed to the dipolar interaction. The contribution of the A_5 term is proportional to the second moment in a system with a three-dimensional spin dynamics.[29] The exchange frequency ω_{ex} is obtained from the value of A_5 using:[27]

$$A_5 = \frac{\sqrt{\pi}}{2\omega_{ex}}$$

where $\omega_{ex}^2 = zJ^2/\hbar^2$, and $z = 2$ is the number of nearest coupled neighbors (Figure 2) with $J = J_{ij}$[12] in eq 5. The residual Zeeman contribution is the same in both compounds but its contribution for compound **I** is negligible in front of the dipolar contribution. The experimental results indicate that the exchange frequency ω_{ex} in compound **I** is greater than in compound **II**. Using the values of A_5 and A_6 (eq 6) obtained from the line width data for compound **I** and **II**, we calculated the values $|J/k| = 118$ mK for $[Cu(\text{L-proline})_2]_2 \cdot 5H_2O$ (**I**) and $|J'/k| = 48$ mK for $Cu(\text{D,L-proline})_2 \cdot 2H_2O$ (**II**).

Exchange Interactions and Superexchange Paths. The relevant superexchange paths between copper ions in compounds **I** and **II** are very different. In $Cu(\text{D,L-proline})_2 \cdot 2H_2O$ (**II**) the EPR experiments do not allow us to evaluate the exchange interaction between magnetically equivalent Cu ions within the layer. The exchange pathway (J') between nonequivalent copper neighbors at 9.47 Å in different layers involves a weak hydrogen bond [Cu(1)−O(3)- - -H−C(4)−C−N−Cu(2)] in an axial−equatorial coupling (see Figure 5). This weak hydrogen bond is formed when the hydrogen atom is covalently bonded to an atom slightly more electroneutral than hydrogen. This interaction, mainly electrostatic, has energies and geometries similar to those of van der Waals complexes. The evidence of a directional involvement of the hydrogen bond may distinguish it from them. The role of this type of bonds in determining molecular configuration or packing in crystals is very important in molecular biology.[30] From the EPR data, the collapse of the resonances of the two nonequivalent copper ions put a lower limit in the magnitude of $|J'/k| \geq 20$ mK, the isotropic exchange between rotated copper ions. We calculated $|J'/k| = 48$ mK from the coefficient A_6 using eq 6. There are not other connections that may contribute to the exchange interaction J' between these copper ions.

In compound **I** pairs of copper ions type A at 7.25 Å are arranged in chains through an axial−equatorial path [$Cu(1_A)$−O−C═O(2)- - -H−Ow_1−$Cu(2_A)$] involving five diamagnetic atoms (see Figure 2). $Cu(1_A)$ and $Cu(2_B)$ in different chains at a distance of 6.64 Å are connected by a path containing seven diamagnetic atoms in an equatorial−equatorial coupling [$Cu(1_A)$−O−C═O(4)- - -H−Ow_4−H−O(5)−$Cu(2_B)$]. These equatorial−equatorial paths, which connect isolated pairs of nonequivalent copper ions, is expected to be more effective than the first one for the transmission of the exchange interaction because the unpaired electron density is mainly concentrated in an in-plane orbital. However, it does not give rise to a three-dimensional spin dynamics by itself in order to produce a narrowing of the resonance. Thus the value $|J/k| = 118$ mK evaluated in our experiment is attributed to the axial−equatorial path.

Conclusions

The values $\mathbf{g}_{\parallel} = 2.245$ (2.252) and $\mathbf{g}_{\perp} = 2.063$ (2.066) obtained for the molecular **g** factors in $[Cu(\text{L-proline})_2]_2 \cdot 5H_2O$ (**I**) and $Cu(\text{D,L-proline})_2 \cdot 2H_2O$ (**II**), respectively (Table 3) reflect the similarity of the local ligand field interaction for Cu(II) ions in each compound expected from the structural data, and indicate that the unpaired electron occupies the $d_{x^2-y^2}$ orbital.[31] The results for $Cu(\text{D,L-proline})_2 \cdot 2H_2O$ may be compared with the rhombic **g** tensor calculated by Hitchman et al.[10] from EPR and polarized electronic spectral data in single crystals. Unfortunately there are no similar electronic spectral data for $[Cu(\text{L-proline})_2]_2 \cdot 5H_2O$ to allow similar calculations of the molecular **g** factors in order to compare with their results. As pointed out before, the orientation of the apical ligands relative to the abc' crystal axis system is similar in compounds **I** and **II** (Figure 4). This is reflected by the observed angular variations of the resonance position, which are similar in both compounds (Figure 6).

The angular variation of the peak-to-peak EPR line width for the two complexes (Figure 7) show important differences that arise from the different exchange networks of compounds **I** and **II**. In $Cu(\text{D,L-proline})_2 \cdot 2H_2O$ (**II**), our data allow to determine the efficiency of a superexchange pathway containing a weak hydrogen bond C−H- - -O to transmit an exchange interaction $|J'/k| = 48$ mK between copper ions at 9.47 Å in an axial−equatorial coupling. In $[Cu(\text{L-proline})_2]_2 \cdot 5H_2O$ (**I**) we evaluated the intermolecular exchange coupling ($|J/k| = 118$ mK) within the chains of copper ions type A. The connection between chains made of coppers type A with coppers type B

---

(28) Levstein, P. R.; Steren, C. A.; Gennaro, A. M.; Calvo, R. *Chem. Phys.* **1988**, *120*, 449.

(29) Richards, P. M.; Salamon, M. B. *Phys. Rev. B* **1974**, *9*, 32.

(30) Jeffrey, G. A.; Saenger, W. In *Hydrogen Bonding in Biological Structures*: Springer: Berlin, 1994; Chapter 10 and references therein.

(31) Zeiger, H. J.; Pratt, G. W. *Magnetic Interactions in Solids*; Oxford University Press: London, 1973.

complete a periodic three-dimensional array. As the exchange coupling constant between copper ions in compound **I** is greater than that compound **II** we conclude that a pathway involving a carboxylate bridge plus an hydrogen bond at 7.25 Å (compound **I**) is more effective than a pathway including a weak hydrogen bond (compound **II**) in the transmission of the superexchange. Hendrickson et al.[32] reviewed data from his group in several compounds where the exchange interactions between metal ions propagate through chemical paths that involve a H bond. The magnitudes of the exchange for cases where the path contains five atoms are comparable to those reported here.

Acknowledgment. This work was supported by UNL (CAI+D 291) and CONICET (PICT-PMT 0055). Support from Fundación Antorchas is gratefully acknowledged.

IC9900758

---

(32) Hendrickson, D. N. In *Magneto Structural Correlations in Exchange-Coupled Systems*; NATO ASI Series; Willet, R. D., Gatteschi, D., Kahn, O., Eds.; Reidel: Dordrecht, 1985; p 523.